Advanced International Journal for Research (AIJFR)
E-ISSN: 3048-7641 ● Website: www.aijfr.com ● Email: editor@aijfr.com

Optimizing of TIG Welding Process for improving tensile strength of ZE41A Magnesium Alloy

A. Ramkumar[1], Shehta E. Abbdou[2]

[1,2] Department of Mechanical Engineering and Technology, Yanbu Industrial College, Royal commission, Yanbu, Kingdom of Saudi Arabia.
Email:[1] ram@rcjy.edu.sa ,[2] abdous1@rcjy.edu.sa

Abstract

This paper reveals an experimental investigation into the influence of welding process parameters of ZE41A magnesium alloy. Experiments are performed, based on Response Surface Method (RSM)- Box Benkhen design. The objective is to understand the effect of welding parameters such as arc current, gas flow rate, and filler metal diameter on the mechanical properties, particularly the hardness and tensile strength, of ZE41A magnesium alloy joints. The performances of the process are evaluated by the hardness and tensile strength of the joint. A second order polynomial regression model has been developed for these input parameters and responses. Analysis of Variance (ANOVA) has been used to test the significance of parameters and adequacy of the developed mode. The confirmation test results prove that the optimal combination of welding parameters achieved from the study improves the performance characteristics of the process.

Keywords: TIG welding, RSM, ANOVA.

1. Introduction

As one of the lightest alloys, magnesium alloys have recently found new interest as engineering materials after having been thoroughly investigated between 1930 and 1960 and hardly at all after that. Especially in the automotive and aerospace industries, their weight-saving potential is important at present. Further advantages are their high processing, machining, and recycling abilities [1-5]. In the manufacturing sectors, welding can be used to join materials and minimize the cost of production. However, it is difficult to weld magnesium alloys to themselves and to other materials. Magnesium alloys are difficult to weld due to their high oxidation tendency, low melting point, and high thermal conductivity, which can lead to porosity, hot cracking, and weld defects. Additionally, when joining with other materials, differences in metallurgical properties often result in weak or brittle joints. It is specifically interesting to prefer the Gas Tungsten Arc Welding (GTAW) technique, which promises to be an economical way to weld magnesium alloy [6]. Although magnesium alloys are challenging to weld, GTAW is preferred due to its precise heat control and use of inert shielding gas, which reduces oxidation and improves weld quality. With proper preheating and surface preparation, GTAW enhances the weldability of magnesium alloys. Presently, the literature about magnesium welding has been

increasing rapidly, mainly focusing on arc welding, laser-beam welding, electron beam welding, and friction-stir welding. For the advantages of utility and economy, GTA welding has been used extensively, and some research on GTA welding has been reported [7-10]. The quality of the weld depends on the selection of parameters and their ranges. It is inevitable to find out optimal process parameters in a minimum experimental run [11]. In this study, the combined effect of TIG welding parameters and post-weld heat treatments (solutionizing and aging) on the mechanical properties of ZE41A magnesium alloy joints was evaluated. While optimization of welding parameters contributed to improved weld quality, the influence of heat treatment on tensile strength cannot be neglected. To solely attribute strength improvements to welding parameters, further evaluation on as-welded samples is required.

AZ31 Mg alloy was welded using automatic tungsten inert gas welding; results revealed weld joints attained efficiency of 84% [12]. In order to improve the quality of the weld, optimizing the weld process is significant. The tensile and shear strength of TIG-welded AZ31B Mg alloy [13] was improved to 29.8% compared to the unoptimized welding condition through process parameter optimization using RSMHybrid RSM-GA was employed to obtain maximum weld strength of seam and spot welds by ultrasonic metal welding [14], the optimal predicted parameter ranges fall very close to validated experimental results. Hybrid RSM-GA combines the statistical modeling capability of Response Surface Methodology (RSM) with the global optimization strength of Genetic Algorithm (GA) to more accurately identify optimal welding parameters. The TIG welding process parameters have been optimized to weld stainless steel S30430 by RSM; ANOVA outcomes elucidate that welding speed was the most significant parameter [15]. RSM has applied to determine the feasible parameter condition of submerged arc welding for coating MgO on St37 steel plate. TIG repair welding causes severe grain growth in the heat-affected zone, which greatly lowers the tensile strength of the repaired joints [16]. Studies on TIG and A-TIG welding of dissimilar AZ61/ZK60 magnesium alloys showed that optimizing current and flux composition significantly refined fusion-zone grains (≈19 μm at 80 A) and enhanced tensile strength (207 MPa), demonstrating the critical role of welding parameters and activating fluxes in strengthening Mg alloy joints [17]. Recent studies on ultrasonic-assisted solid-state welding of thin Mg alloys demonstrated that minimizing heat input and controlling intermetallic evolution can nearly eliminate the HAZ, refine grains (~10 μm), and achieve tensile-shear strength up to 97.8% of the base metal, highlighting the importance of heat management for improving joint strength in Mg alloys [18].

In this study, an experiment was conducted using the RSM-Box Behnken design to analyze the influence of key TIG welding parameters—arc current, gas flow rate, and filler metal diameter—on the mechanical properties of ZE41A magnesium alloy joints. The primary aim is to develop a predictive model and optimize the process parameters to maximize tensile strength and hardness of the welded joints. Statistical tools such as ANOVA and regression analysis are employed to determine the significance of each parameter and validate the model's adequacy.

2. Experimental Study

2.1 Welding Process Parameter Selection

The ZE41A magnesium alloy is composed of 3.5-5 wt% Zn, 0.8-1.7 wt% RE, 0.4-1 wt% Zr, and the remaining wt% magnesium. The alloy is made by the casting route with a sand mould. Welding plates are machined to the size of 90mm X 80mm X 6mm and welding experiments are conducted using the gas tungsten arc welding (GTAW) method. The filler metal is cut from the base plate size of 310mm

X 210mm X 8mm and has the same composition of the base metal. To obtain optimal welding parameters, welding experiments are carried out by setting the arc current ranging from 175 to 225 A, gas flow rate of 15 to 19 L/min, and filler rod diameter of 4 to 5mm [19]. Edges to be joined are designed to be single V with 1mm root thickness. Edges to be joined are designed to a single V-groove with a groove angle of 60° and a root thickness of 1 mm. The leftward welding technique is followed, and two passes are sufficient to fill up the gap. In order to prevent weld cracking, the welding plates are preheated to 200°C. After the completion of the welding process, the welded plate for these experiments is heat-treated by solutionizing at a temperature of 330°C for 2 hrs to improve the strength, toughness, and shock resistance of the magnesium alloy. Figure 1 displays a representative welded specimen; optimization was determined based on mechanical test results rather than visual inspection alone. The aging is done after solutionizing treatment of magnesium alloy at 180°C for 16 hrs to improve hardness and strength [20].

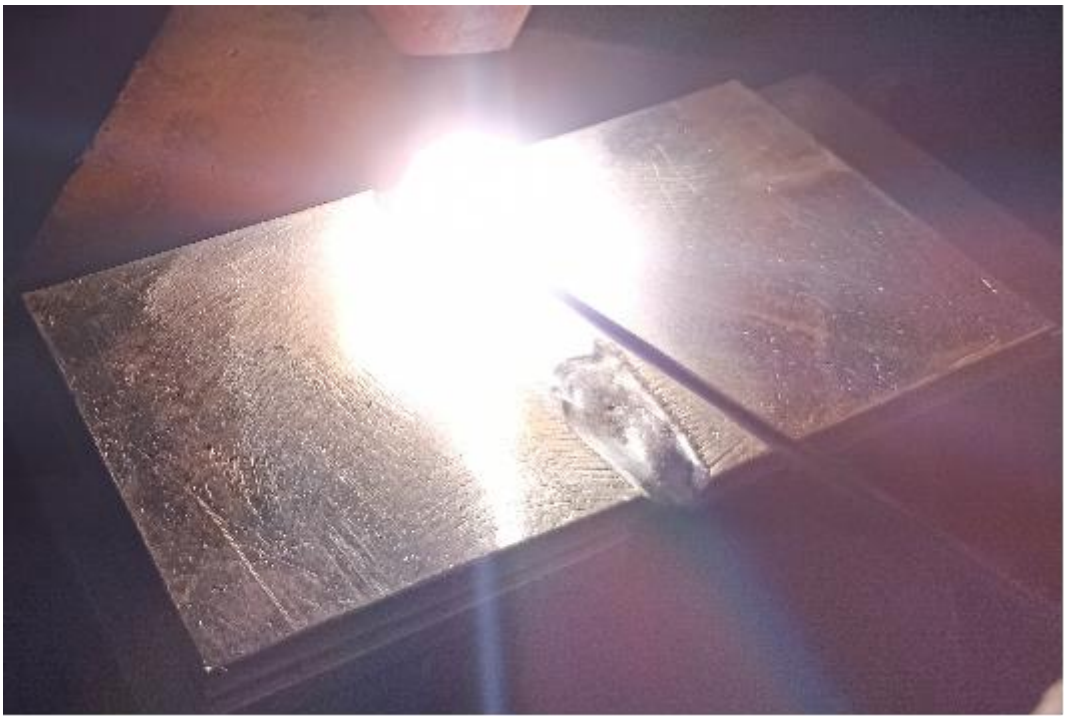

Fig.1 Welded material at optimal condition

2.2 Selection of Design Matrix

In this study, the process parameter levels and RSM - Box Benkhen design matrix was chosen as per standards recommended by the design of experiments and their levels are given in Table.1. The 15 experimental run for three parameters and three levels are selected. The Minitab software is used to design experimental matrix and statistical analysis.

Table.1 Design of Experiment for weld ZE41A Mg alloy

Exp. Run	Arc Current (A)	Gas Flow Rate (L/min)	Filler Diameter (mm)
1.	200	15	4.0
2.	200	17	3.5
3.	175	19	3.5
4.	175	17	4.0
5.	200	17	3.5
6.	175	17	3.0
7.	225	17	4.0
8.	175	15	3.5
9.	200	17	3.5
10.	225	17	3.0
11	200	19	3.0
12	200	19	4.0
13.	200	15	3.0
14.	225	19	3.5
15.	225	15	3.5

2.3 Welding Performance Evaluation

The welding performance is evaluated by tensile testing and microhardness measurement. The tensile and hardness samples are machined from the transverse direction of the weld (the weld in the center of the gauge length in the tensile specimen). The cylindrical specimens for the tension test conform to the standard specified in ASTM E8 with a gauge length that measures 30 mm in length and 6 mm in diameter. The tensile tests are carried out in an FIE servo controlled universal testing machine. The tensile tests are carried out at room temperature and at a strain rate of 0.05 s^{-1}. Samples for hardness testing are cut from the nugget part, and the surfaces are polished. The hardness tests are carried out at hardness testers using a Vickers indenter made of sapphire, and provisions for testing have been developed.

3. Regression Model

The second-order polynomial model [21, 22] can be developed between input parameters and output responses. The appropriate experimental designs with accurate data could be used for parameter predictions. It is assumed that for n runs of experiments, the second-order equation (3) is formed as:

$$y_i = \beta_o + \sum_{j=1}^{f} \beta_j x_j + \sum_{j<k}^{f} \beta_{jk} x_j x_k + \sum_{j=1}^{f} \beta_{jj} x_j^2 + \epsilon \quad \text{---- (1)}$$

Where Yi represents the performance of the ith of n experimental runs, xi is the parameter level for the jth parameter, βo represents the intercept, βj is the linear effect of the jth factor, βjk represents the interaction between the jth and kth factors, and βjj stands for the quadratic of the jth factor. ε is a normally distributed error.

To simplify the generated modeling, Arc Current is representing as 'AC', Gas Flow Rate as 'GF' and Filler Diameter as 'FD'.

4. Results and Discussion

Table 2 represents the input parameter combination and its responses measured through hardness and tensile tests. The maximum tensile strength (UTS) of 167 MPa has been attained at an arc current of 200 A, a gas flow rate of 19 L/min, and a filler diameter of 3 mm. Moreover, maximum hardness of 72 HV was measured for an arc current of 225 A, a gas flow rate of 17 L/min, and a filler diameter of 4 mm.

Table.2 Experimental Results Measured

Exp. Run	Arc Current (A)	Gas Flow Rate (L/min)	Filler Diameter (mm)	UTS (MPa)	Hardness (HV)
1.	200	15	4.0	146	66.2
2.	200	17	3.5	158	67.0
3.	175	19	3.5	135	62.0
4.	175	17	4.0	132	61.0
5.	200	17	3.5	164	67.4
6.	175	17	3.0	135	64.0
7.	225	17	4.0	153	72.0
8.	175	15	3.5	141	60.2
9.	200	17	3.5	161	68.2
10.	225	17	3.0	143	70.0
11	200	19	3.0	167	69.0
12	200	19	4.0	158	67.0
13.	200	15	3.0	149	67.8
14.	225	19	3.5	136	71.0
15.	225	15	3.5	131	71.4

4.1 Hardness

The developed regression model for the hardness is given below as equation (2) as a function of coded units.

$$\text{Hardness} = -19.8667+0.7057*AC+GF*504542-27.3833*FD-0.0017*AC*AC- 0.0792*GF*GF + 1.1333FD*FD-0.0110*AC*GF+0.1*AC*FD-0.1*GF*FD \quad \text{----- (2)}$$

Where:
AC = Arc Current (A)
GF = Gas Flow Rate (L/min)
FD = Filler Diameter (mm)

The regression model for hardness was tested by ANOVA to check the adequacy and is summarized in Table 3. The F ratio greater than 4 and the P value less than 0.005 show that the model is statistically significant [23]. The predicted R^2 shows 98.5% adequacy for the developed model. The p-value of the regression model is 0.001; hence, the model is fitted to the experimental value.

Table.3 ANOVA of the regression model for Hardness (Hv)

Source	DF	Seq SS	Adj SS	Adj MS	F	P
Regression	9	189.521	189.5207	21.0579	36.10	0.001
Linear	3	177.070	7.5930	2.5310	4.34	0.074
Square	3	4.951	4.9507	1.6502	2.83	0.146
Interaction	3	7.500	7.5000	2.5000	4.29	0.076
Residual Error	5	2.917	2.9167	0.5833		
Lack-of-Fit	3	2.170	2.1700	0.7233	1.94	0.358
Pure Error	2	0.747	0.7467	0.3733		
Total	14	192.437				

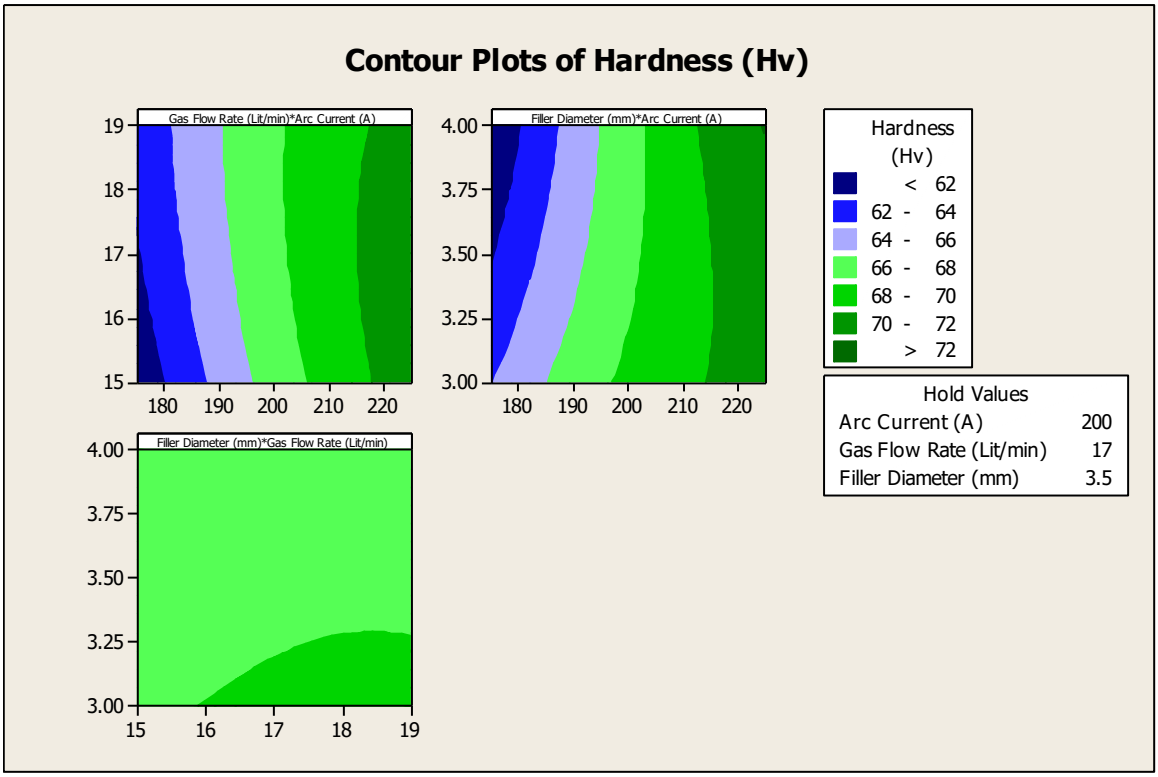

Fig.2 Contour Plot for Hardness (Hv)

- **X**-axis: Arc Current (A)
- **Y**-axis: Gas Flow Rate (L/min) or Filler Diameter (mm) *(depending on the variable pairing used in the plot)*

 Z-axis / Contour Legend: Hardness (HV)

The contour plot for the hardness is represented in Figure 2. It is observed that at a maximum arc current of 225 A, irrespective of gas flow rate and filler diameter levels, hardness increased a maximum of 72 Hv. The low hardness value of below 62 Hv has been attained at low arc current with respect to low gas flow rate and higher filler diameter. The nominal hardness value of 66 to 70 Hv has been achieved with an arc current between 195 and 210 A.

4.2 Ultimate Tensile Strength

Table.4 Analysis of Variance for UTS (MPa)

Source	DF	Seq SS	Adj SS	Adj MS	F	P
Regression	9	2745.18	2745.18	793.909	42.67	0.002
Linear	3	158.25	795.59	265.196	3.65	0.099
Square	3	1505.43	1505.43	501.811	6.90	0.032
Interaction	3	81.50	81.50	27.167	0.37	0.776
Residual Error	5	363.75	363.75	72.750		
Lack-of-Fit	3	345.75	345.75	74.250	1.81	0.073
Pure Error	2	18.00	18.00	9.000		
Total	14	3108.93				

The developed regression model for the ultimate tensile strength is given below as equation (3) as a function of coded units.

UTS = -1291.56+10.89*AC+42.81*GF-13.75*FD-0.03*AC*AC-1.37*GF*GF-2*FD*FD
+0.06*AC*GF+ 0.26*AC*FD-1.5*GF*FD ---------- (3)

Where:
AC = Arc Current (A)
GF = Gas Flow Rate (L/min)
FD = Filler Diameter (mm)
The developed regression model for ultimate tensile strength was tested by ANOVA to verify the adequacy and is summarized in Table 4. The F ratio falls greater than 4, and a P value less than 0.005 shows that the model is statistically significant. The predicted R^2 shows 92.3% adequacy for the developed model. The p-value of the regression model is 0.001; hence, the model is fitted to the experimental value.

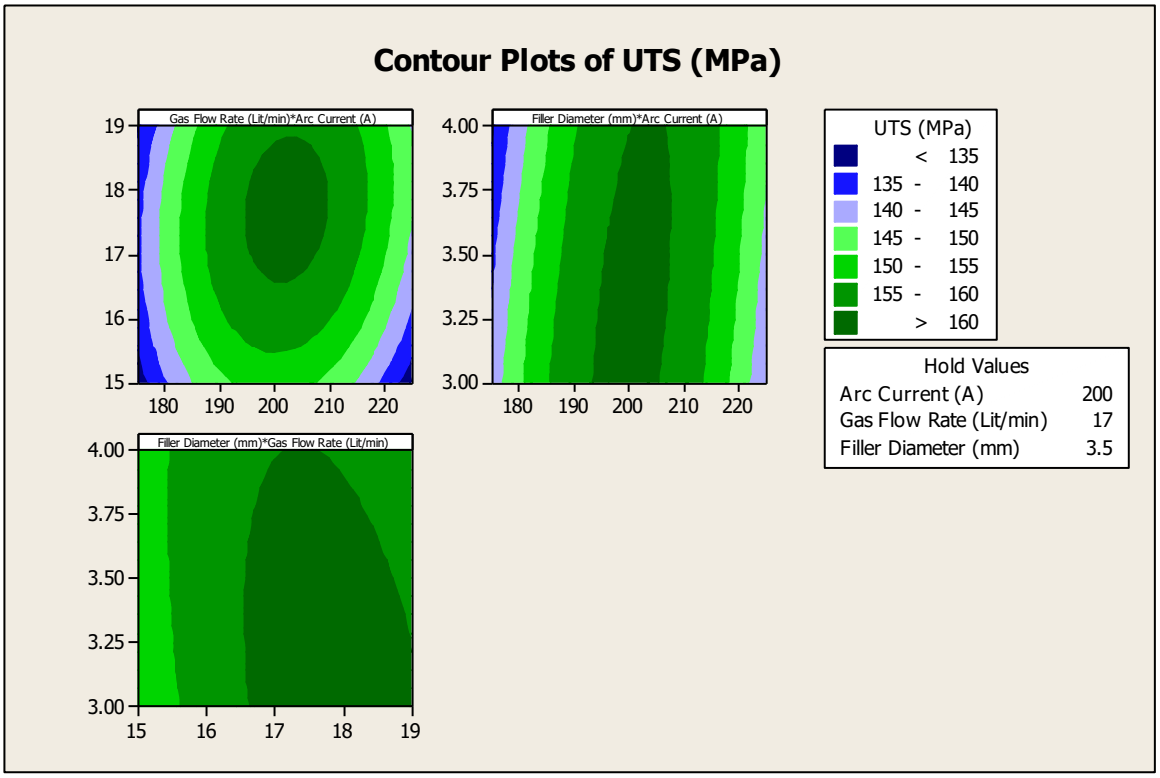

Fig.3 Contour Plot for Ultimate Tensile Strength (MPa)

- X-axis: Arc Current (A)
- Y-axis: Gas Flow Rate (L/min) or Filler Diameter (mm) *(based on plot pairing)*
- Z-axis / Contour Legend: Tensile Strength (MPa)

Fig. 3 shows the contour plot for ultimate tensile strength. The arc current between 185A and 215A exhibits better tensile strength when gas flow is between 17 and 18 L/min and filler diameter is 3 to 3.5 mm. The arc current is below 185A and above 215A; irrespective of gas flow rate and filler diameter, the tensile strength reduces to below 145 MPa.

4.3 Optimization

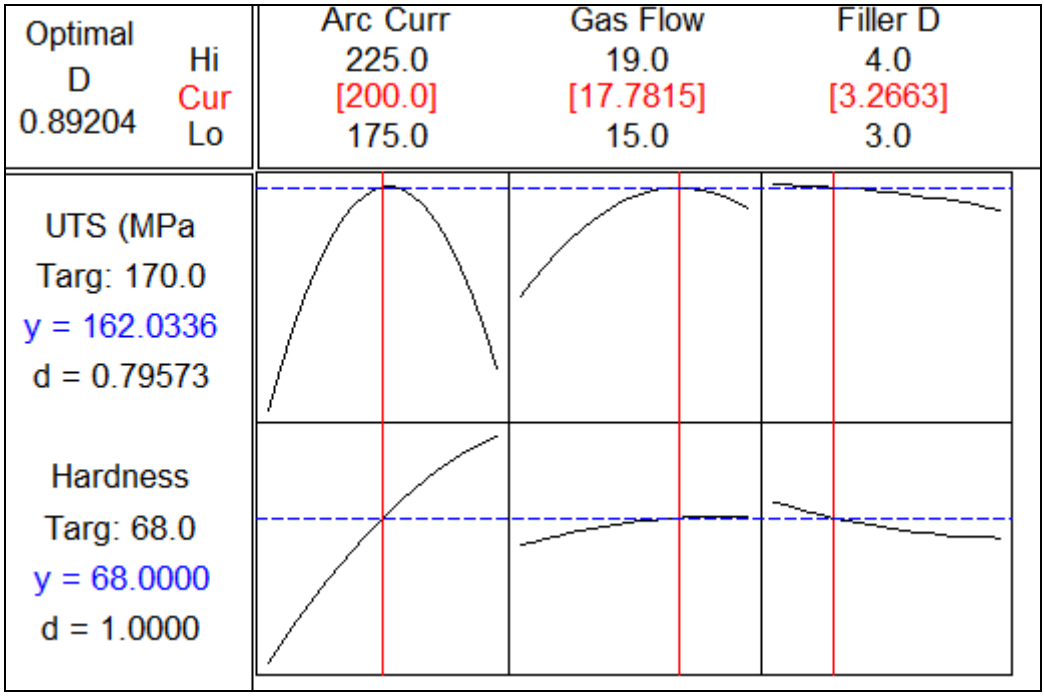

Fig.4 Influence of Input Parameters for Optimal Condition

Fig. 4 illustrated the optimal parameter conditions at which better responses are obtained. It is predicted that an arc current of 200 A, a gas flow rate of 17.7815 L/min, and a filler diameter of 3.2663 mm resulted in better responses of 172 MPa tensile strength and 68 Hv hardness value. The desirability of the optimal condition attained 89%. This shows the predicted input condition can yield higher output responses.

5. Conclusions

This study investigated the effects of TIG welding process parameters—arc current (AC), gas flow rate (GF), and filler diameter (FD)—on the mechanical properties (tensile strength and hardness) of ZE41A magnesium alloy joints, using Response Surface Methodology (RSM) and ANOVA for statistical modeling and optimization.

- A second-order polynomial regression model was developed and validated using ANOVA, confirming its statistical significance and high predictive capability for both tensile strength and hardness.
- Among the parameters studied, arc current was identified as the most influential factor affecting both mechanical properties.
- The optimal combination of process parameters (AC = 200 A, GF = 17.78 L/min, FD = 3.26 mm) yielded a predicted tensile strength of 162 MPa and hardness of 68 Hv, with a desirability of 89%.
- The results reflect the combined effects of welding parameters and post-weld heat treatment, suggesting that while parameter optimization enhances joint performance, further evaluation on as-welded samples is needed to isolate the effect of welding conditions alone.

Thus, the study successfully achieved its objective of modeling and optimizing TIG welding parameters for enhanced mechanical performance of ZE41A magnesium alloy welds.

Reference

1. Froes, F.H., Kim, Y.W., Krishnamurthy, S., 1989. Rapid solidification of lightweight metal alloys. *Mater. Sci. Eng. A* 117, 19–32.
2. Smith, W.E., 1993. *Structure and Properties of Engineering Alloys*. McGraw Hill, New York.
3. Mordike, B.L., Ebert, T., 2001. Magnesium properties–application–potential. *Mater. Sci. Eng. A* 302, 37–42.
4. Eacherath, S., Murugesan, S., 2018. Synthesis and characterization of magnesium-based hybrid composites – A review. *Int. J. Mater. Res.* 109(7), 661–672.
5. Sivapragash, M., Kumaradhas, P., Stanly Jones Retnam, B., Vettivel, S.C., 2018. Optimization of PVD process parameter for coating AZ91D magnesium alloy by Taguchi grey approach. *J. Magnes. Alloy* 6(2), 171–179.
6. Song, G., Diao, Z., Lv, X., Liu, L., 2018. TIG and laser–TIG hybrid filler wire welding of casting and wrought dissimilar magnesium alloy. *J. Manuf. Process.* 34, 204–214.
7. Carlone, P., Palazzo, G.S., 2015. Characterization of TIG and FSW weldings in cast ZE41A magnesium alloy. *J. Mater. Process. Technol.* 215, 87–94.
8. Zhou, M., Shen, J., Hu, D., Gao, R., Li, S., 2017. Effects of heat treatment on the activated flux TIG-welded AZ31 magnesium alloy joints. *Int. J. Adv. Manuf. Technol.* 92, 3983–3990.
9. Carlone, P., Astarita, A., Rubino, F., Pasquino, N., 2016. Microstructural aspects in FSW and TIG welding of cast ZE41A magnesium alloy. *Metall. Mater. Trans. B* 47B, 1340–1346.
10. Wang, H., Song, G., 2016. Influence of adhesive and Ni on the interface between Mg and Fe in the laser-TIG-adhesive hybrid welding joint. *Int. J. Precis. Eng. Manuf.* 17(6), 823–827.
11. Ajith, P.M., Afsal Husain, T.M., Sathiya, P., Aravindan, S., 2015. Multi-objective optimization of continuous drive friction welding process parameters using response surface methodology with intelligent optimization algorithm. *J. Iron Steel Res. Int.* 22(10), 954–960.
12. Liu, H.T., Zhou, J.X., Zhao, D.Q., Liu, Y.T., Wu, J.H., Yang, Y.S., Ma, B.C., Zhuang, H.H., 2017. Characteristics of AZ31 Mg alloy joint using automatic TIG welding. *Int. J. Miner. Metall. Mater.* 24(1), 102–108.
13. Salleh, M.N.M., Ishak, M., Quazi, M.M., Aiman, M.H., 2018. Microstructure, mechanical, and failure characteristics of laser-microwelded AZ31B Mg alloy optimized by response surface methodology. *Int. J. Adv. Manuf. Technol.* 99, 985–1001.
14. Elangovan, S., Anand, K., Prakasan, K., 2012. Parametric optimization of ultrasonic metal welding using response surface methodology and genetic algorithm. *Int. J. Adv. Manuf. Technol.* 63, 561–572.
15. Ahmad, A., Alam, S., 2019. Parametric optimization of TIG welding using Response Surface Methodology. *Mater. Today Proc.* 18, 3071–3079.
16. Lei Wang., Zhengtao Liu., Yicheng Feng., YuanKe Fu., Sicong Zhao., Erjun Guo.,2025 Effect of TIG repaired welding process on microstructure and mechanical properties of as-cast Mg-4Y-3Nd-1.5Al alloy. Materials Characterization 219, 114622.

17. Bo QIN., Fu-cheng YIN., Cheng-zong ZENG., Jia-cheng XIE., Jun SHE.,2019. Microstructure and mechanical properties of TIG/A-TIG welded AZ61/ZK60 magnesium alloy joints.Transactions of Nonferrous Metals Society of China, 29(9), 1864–1872.
18. Yanfei Chen., Zhengqiang Zhu., M. Amir Siddiq., Ke Li., Fanrong Ai., Zhigang Wang., 2025.Minimal strength loss and corresponding mechanisms in the ultrasonic joining of magnesium alloys. Materials Science and Engineering: A, 934, 148346.
19. Sivapragash, M., Lakshminarayanan, P.R., Karthikeyan, R., Raghukandan, K., Hanumantha, M., 2007. Fatigue life prediction of ZE41A magnesium alloy using Weibull distribution. Mater. Des. 29(8), 1549–1553.
20. Rajan, T.V., Sharma, C.P., Sharma, A., 1988. *Heat Treatment Principles and Techniques*. Prentice-Hall of India, New Delhi.
21. Murugan, N., Kumar, B.A., 2014. Prediction of tensile strength of friction stir welded stir cast AA6061-T6/AlNp composite. *Mater. Des.* 51, 998–1007.
22. Elangovan, K., Balasubramanian, V., Babu, S., 2012. Predicting tensile strength of friction stir welded AA6061 aluminium alloy joints by a mathematical model. *Mater. Des.* 30(1), 188–193.
23. Kumar, S.S., Murugan, N., Ramachandran, K.K., 2019. Identifying the optimal FSW process parameters for maximizing the tensile strength of friction stir welded AISI 316L butt joints. *Measurement* 137, 257–271.